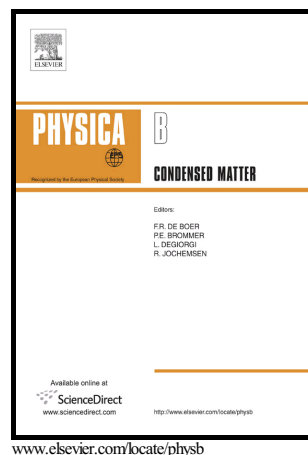


## Author's Accepted Manuscript

Growth and characterization of an efficient new NLO single crystal L-phenylalanine D-methionine for frequency conversion and optoelectronic applications

P. Sangeetha, P. Jayaprakash, M. Nageshwari, C. Rathika Thaya Kumari, S. Sudha, M. Prakash, G. Vinitha, M. Lydia Caroline



PII: S0921-4526(17)30522-7  
DOI: <http://dx.doi.org/10.1016/j.physb.2017.08.037>  
Reference: PHYSB310177

To appear in: *Physica B: Physics of Condensed Matter*

Received date: 8 July 2017  
Revised date: 15 August 2017  
Accepted date: 16 August 2017

Cite this article as: P. Sangeetha, P. Jayaprakash, M. Nageshwari, C. Rathika Thaya Kumari, S. Sudha, M. Prakash, G. Vinitha and M. Lydia Caroline, Growth and characterization of an efficient new NLO single crystal L-phenylalanine D-methionine for frequency conversion and optoelectronic applications, *Physica B: Physics of Condensed Matter*, <http://dx.doi.org/10.1016/j.physb.2017.08.037>

This is a PDF file of an unedited manuscript that has been accepted for publication. As a service to our customers we are providing this early version of the manuscript. The manuscript will undergo copyediting, typesetting, and review of the resulting galley proof before it is published in its final citable form. Please note that during the production process errors may be discovered which could affect the content, and all legal disclaimers that apply to the journal pertain.

**Growth and characterization of an efficient new NLO single crystal  
L-phenylalanine D-methionine for frequency conversion and optoelectronic applications**

P. Sangeetha<sup>1</sup>, P. Jayaprakash<sup>1</sup>, M. Nageshwari<sup>1</sup>, C.Rathika Thaya Kumari<sup>1</sup>, S. Sudha<sup>1</sup>, M.Prakash<sup>3</sup>,

G. Vinitha<sup>4</sup>, M. Lydia Caroline<sup>1,2\*</sup>

<sup>1</sup>PG & Research Department of Physics, Arignar Anna Govt. Arts College, Cheyyar - 604 407,  
Tamil Nadu, India

<sup>2</sup>Department of Physics, Dr Ambedkar Govt. Arts College, Vysarpadi, Chennai – 600 039,  
Tamil Nadu, India

<sup>3</sup> PG & Research Department of physics, Urumu Dhanalakshmi College, Thiruchirappalli - 19,  
Tamil Nadu, India

<sup>4</sup>Department of Physics, School of Advanced Sciences, VIT, Chennai – 600127, Tamil Nadu, India

**Abstract:**

Optically active single crystals of L-phenylalanine D-methionine (LPDM) were grown by slow evaporation technique by co-crystallization of amino acids L-phenylalanine and D-methionine in water. The unit cell dimensions have been identified from single crystal X-ray diffraction technique. The existences of various hydrocarbyls were examined by FTIR and FT-Raman spectroscopy. The carbon and hydrogen environment of the grown crystals were analysed by FT-NMR spectrum. The optical absorption studies show that the crystal is transparent in the visible region with a lower cut-off wavelength of 259 nm and there by optical band gap energy  $E_g$  is calculated to be 5.35 eV. The Urbach energy, extinction coefficient, reflectance were calculated from UV-absorption data. Further, the thermal stability and accurate melting point has been investigated by TG/DSC techniques. The Kurtz powder SHG was confirmed using Nd:YAG laser with fundamental wavelength of 1064 nm. The dielectric behavior of the specimen has been determined for various temperatures (313 K, 333 K, 353 K, 373 K) at different frequencies. Fluorescence study and the time resolved decay calculation was

also performed for the LPDM crystal. Optical nonlinear susceptibility was measured in LPDM and the real and imaginary part of  $\chi^3$  was evaluated by Z-scan technique using open and closed apertures.

**Keywords:** Nonlinear optical material; X-ray diffraction; optical properties; dielectric; fluorescence; third harmonic generation.

**Corresponding author Email address and mobile no:**

lydiacaroline2006@yahoo.co.in(M.Lydia Caroline);

Tel: 044-25520151: Fax: 044 - 2552 1852

+91 9841720216

## 1. Introduction

From the past few decades it was observed that the amino acid based compounds have potential nonlinear optical (NLO) behavior and disclose good mechanical strength [1]. Nonlinear optical materials are proved to be a suitable candidate for photonics and optoelectronic industries [1]. These materials are efficiently utilized for frequency conversion, optical switching, device fabrication, and large capacity communications because, further application of these may be provided in all optical systems. Among organic and inorganic materials, the organic one shows extremely outstanding characteristics of NLO behavior due to weak Vander Waals forces and hydrogen bonds with conjugate  $\pi$  electrons [1]. Amino acids based materials catches the attention in the field of NLO applications as they contain a proton donor carboxylic acid (COOH) group and the proton acceptor amino ( $\text{NH}_2$ ) group in them [2]. Nowadays crystallization is one of the most important separation and purification processes in the pharmaceutical and chemical industries. One method for race mate separation is “resolution by entrainment”, which is usually referred to as preferential crystallization also adopted for growing

nonlinear optical crystals [3]. Anisotropic L-phenylalanine has many different positive effects anxiety relief with increased focus and concentration, and improved motivation [4]. Methionine is one of the sulfur containing amino acid which it is structurally different from other amino acids. Optically active methionine is required in the human diet for normal metabolism and growth, since it is synthesized in humans. D-methionine is often used as an additive in animal feedstuffs, and it is also used in production of medicines and active pharmaceutical ingredients, and as a precursor to other amino acids [3]. The growth and characterization of complexes of L-phenylalanine single crystals were reported in the literature earlier [5-7]. L-phenylalanine D-methionine (LPDM) is the simplest acentric member of the family crystallized by Yamamoto et al [8]. Our present work was carried out to harvest optically clear crystals from L-phenylalanine and D-methionine taken in the equimolar ratio (1:1) and to extent our work to linear and nonlinear optical studies to prove its suitability for photonic applications. The peptide (LPDM) includes hydrogen bond donors and acceptors in the peptide bonds in addition to the C-terminal-COO<sup>-</sup> carboxylate group and the N-terminal -NH<sub>3</sub><sup>+</sup> amino group [9]. Already the stoichiometric crystallization of the title compound was studied by Gorbitz et al [10]. Also much interest has been concentrated on organic materials as third-order nonlinear optical materials among which some organic materials with conjugated  $\pi$ -electrons show remarkably large nonlinearities [11,12]. Since several third order nonlinear optical materials show intensity dependent refractive indices since they evince fast response time and low absorption [13]. Here by we report various characterizations for the grown specimen including SXRD, UV-absorption studies, FTIR, FT-Raman, FT-NMR, Fluorescence and Life time, dielectric studies, second (SHG) and third harmonic generation (THG) studies suitable for opto electronics and NLO applications.

## 2. Materials and methods

The commercially available raw materials L-phenylalanine (LOBA, 99%) and D-methionine (LOBA, 99%) in the purest form were taken in an equimolar (1:1) ratio and dissolved in the double distilled water. After continuous stirring for 8 h at room temperature homogenous saturated solution was obtained which was then filtered in the vessel using whatman filter paper at room temperature. After a time span of 30 days optically good quality crystals were harvested from the mother solution by solution evaporation method. The chemical reaction is depicted in Fig.1. The crystallization of L-phenylalanine with D-methionine produced good quality crystals finds suitable for enhanced nonlinear optical efficiency in the field of nonlinear optical applications. The photograph of grown crystals of LPDM is shown in Fig.2.

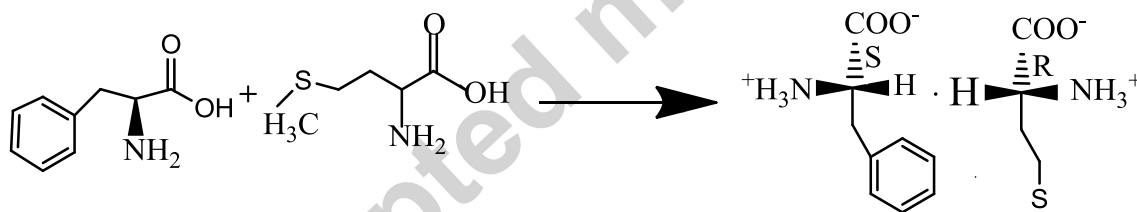


**Fig.1. Reaction scheme for LPDM compound.**

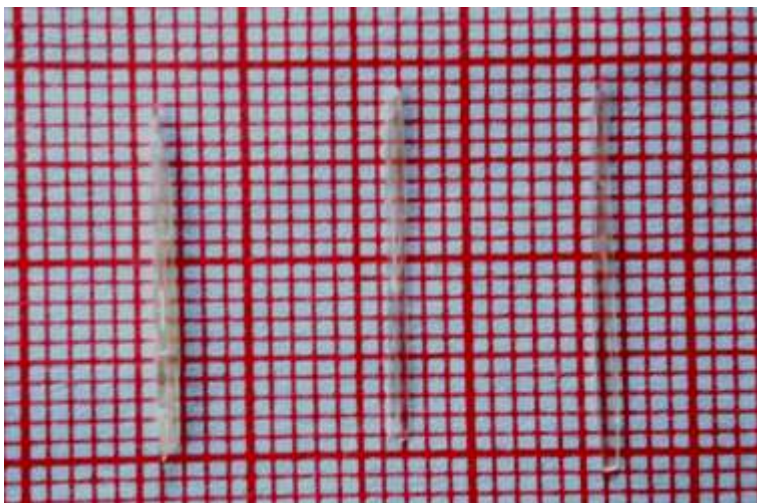


**Fig.2. Photograph of single crystals of LPDM grown slow evaporation method**

### **2.1. Characterization studies**

The grown L-Phenylalanine D-methionine crystal was subjected to various characterization techniques like single crystal X-ray diffraction, Fourier Transform Infra-Red (FTIR), Fourier Transform Raman (FT-Raman) vibrational, UV-visible spectral, Nuclear Magnetic Resonance (NMR), TG/DSC, Nonlinear Optical (NLO) study, Fluorescence lifetime and dielectric studies. BRUKER KAPPA APEX II CCD diffractometer with MoK $\alpha$  ( $\lambda=0.71073\text{\AA}$ ) radiation was utilized to measure the cell dimensions. FTIR spectrum was recorded using PERKIN ELMER spectrometer in the range  $4000-400\text{cm}^{-1}$  by KBr pellet technique. Powder FT-Raman spectrum was recorded on a BRUKER: RFS 27 spectrometer in the range  $4000-450\text{cm}^{-1}$ . A BRUKER AMX 400 spectrometer was utilized to study the carbon-hydrogen frame work in the molecule using DMSO as solvent. UV-visible absorption spectrum was recorded in the region 200-700 nm using PERKIN ELMER LAMADA 35 spectrophotometer. The TG/DSC of LPDM has been recorded by using NETZSCH STA 449F3

thermal analyzer at a heating rate of  $20^{\circ}\text{C min}^{-1}$  in the temperature range of  $20\text{-}1000^{\circ}\text{C}$ . With the performance of PERKIN ELMER LS-45 spectrofluorophotometer using a continuous 450 W xenon lamp excitation source, fluorescence spectrum was obtained in the range of 240-800 nm. The dielectric loss and dielectric constant as a function of frequency for the temperatures 313K, 333K, 353K and 373K were studied using a HIOKI 3532-50 LCR HiTESTER meter. The surface exploration of LPDM was inspected accomplishing FE1 quanta FEG 200 High resolution scanning electron microscope with acceleration voltage of 20KV. To analyze the nonlinear optical property of LPDM powder a pulsed Nd:YAG laser was employed using Kurtz Perry powder method. The third order nonlinearity for LPDM was analyzed by the method of Z-scan using 632.8 nm diode pumped CW Nd-YAG laser.

### **3. Results and discussion**

#### **3.1. Single crystal X-ray diffraction**

From single crystal X-ray diffraction analysis, it was confirmed that the crystal belongs to monoclinic system with noncentrosymmetric space group  $P2_1$ . The attained lattice parameters are presented in Table1. The unit cell parameters are found to be consistent with the reported crystallographic structure data [10].

**Table 1**

Single crystal XRD data of LPDM.

Cell parameters	Present work Monoclinic	Reported work [10] Monoclinic
Space group	P2 <sub>1</sub>	P2 <sub>1</sub>
a (Å)	10.16	10.11
b (Å)	4.75	4.70
c (Å)	16.83	16.68
$\beta$ (°)	106.74	106.66
Volume (Å <sup>3</sup> )	778	760.6

### 3.2. Fourier transform infra-red and Fourier transform Raman vibrational studies

FTIR and FT-Raman spectrum was qualitatively analyzed to know the vibrational interactions of distinct functional groups and the corresponding spectra recorded for LPDM are shown in Fig.3 (a) and Fig.3 (b) respectively. The description on IR absorption reports of L-phenylalanine is well understood in the literature [14-16]. The FTIR wave number observed at 3438 cm<sup>-1</sup> is assigned to O-H stretching carboxylic acid vibration of COOH group [14]. The FT-Raman peaks observed at 3055 cm<sup>-1</sup> is attributed to NH<sub>3</sub><sup>+</sup> asymmetric stretching [15]. The CH<sub>2</sub> stretching is found to appear at 2928 cm<sup>-1</sup> and 2914 cm<sup>-1</sup> respectively in FTIR and FT-Raman spectra. The wave numbers 2084 cm<sup>-1</sup> and 2090 cm<sup>-1</sup> gives CH stretching vibration in IR and Raman spectra [17]. The FTIR and FT-Raman counterpart shows C=O stretching vibrations at 1605 cm<sup>-1</sup> and 1606 cm<sup>-1</sup> respectively. The peaks at 1441 cm<sup>-1</sup> in IR and FT-Raman in 1442 cm<sup>-1</sup> are assigned to COO<sup>-</sup> symmetric stretching in Raman. The wave numbers 1336 cm<sup>-1</sup> and 1338 cm<sup>-1</sup> indicate the presence of aromatic vibrations both in IR and Raman spectrum [16]. The C-N stretching vibrations observed depicted the presence of phenylalanine ions at 1207 cm<sup>-1</sup> and 1249 cm<sup>-1</sup> in

IR and Raman spectra counterpart [16]. The peaks seen at around  $1070\text{ cm}^{-1}$ ,  $1153\text{ cm}^{-1}$ ,  $1065\text{ cm}^{-1}$  and  $1156\text{ cm}^{-1}$  illustrate the C-C aromatic stretching respectively in both spectra. The bands at  $867\text{ cm}^{-1}$  and  $855\text{ cm}^{-1}$  are due to deformation of benzene ring. The intense sharp band at  $766$  and  $743$  establishes the presence of  $\text{CH}_2$  rocking vibration in both spectra [14]. The bands at  $484\text{ cm}^{-1}$  and  $483\text{ cm}^{-1}$  are attributed due to C-C deformation in both IR and FT-Raman spectra. Thus, the presence of all the functional groups present in LPDM was confirmed.

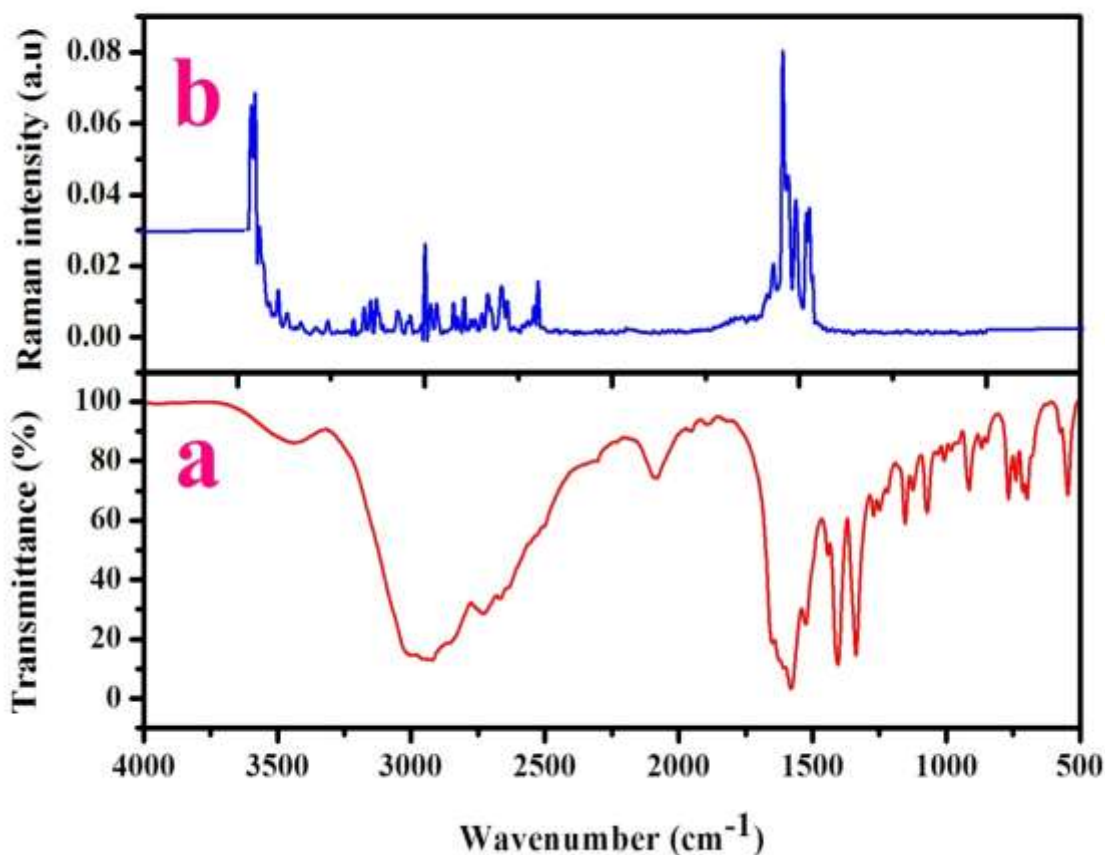


**Fig. 3.** (a) FTIR spectrum and (b) FT-Raman Spectrum of LPDM.

### 3.3. FT-NMR spectral analysis

The analysis of carbon hydrogen network is performed by suitably applying  $^1\text{H}$  and  $^{13}\text{C}$  NMR analytical technique. These techniques are used to identify and confirm the structure of organic compounds. Herewith, the  $^1\text{H}$  NMR spectrum of LPDM crystal recorded is presented in Fig.4. The sharp resonance peak at  $\delta=2.5$  ppm could be attributed due to CH proton of D-methionine. The multiplets that appears in the range 7.20-7.34 ppm shows with less intensity confirms the presence of phenolic protons in the L-phenylalanine (aromatic) aminoacid [18]. The chemical shift seen at  $\delta= 3.6$  ppm could be assigned to proton environment in the amino group ( $\text{NH}_3^+$ ) in both L-phenylalanine and D-methionine residues. The  $^{13}\text{C}$  NMR spectrum of LPDM is depicted in Fig. 5. The  $^{13}\text{C}$  NMR spectrum shows signals in the region 39.5-40.5 ppm which is an indicative of different carbon environment in amino acid D-methionine (aliphatic) [19]. The presence of carbon atom in the phenolic ring of L-phenylalanine is confirmed due to the appearance of resonance peaks at 128.8 ppm and 129.8 ppm respectively.

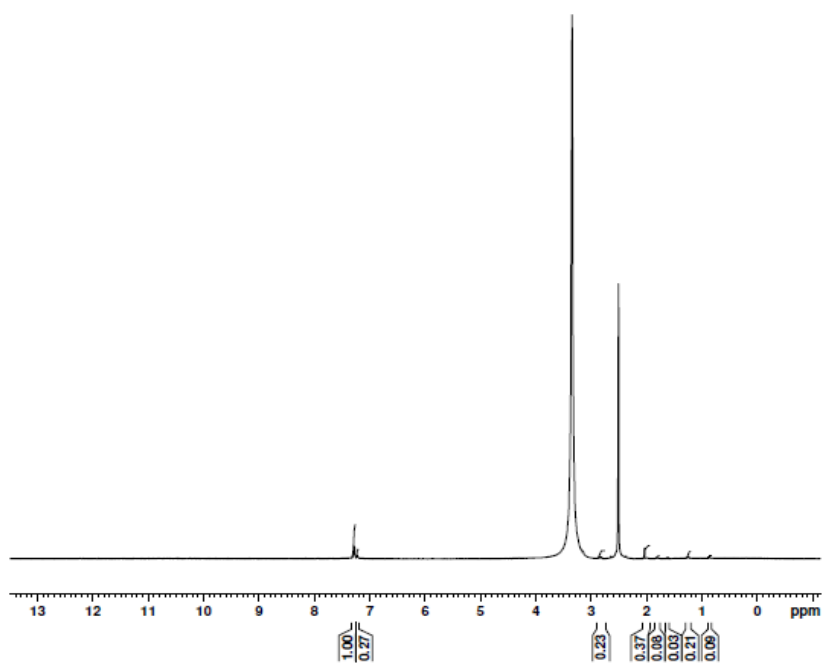


Fig. 4.  $^1\text{H}$  NMR profile of LPDM

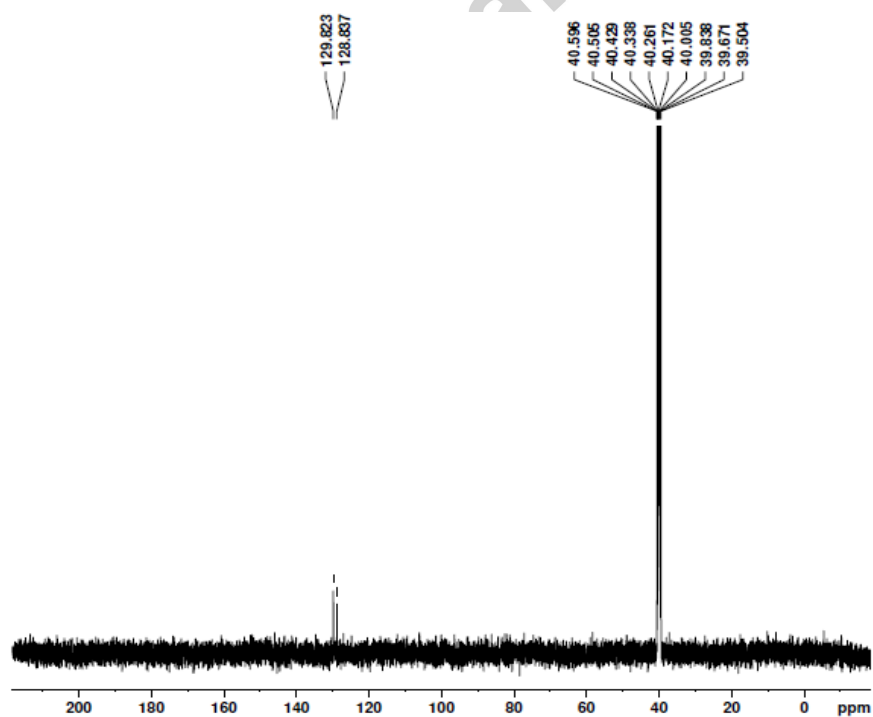


Fig. 5.  $^{13}\text{C}$  NMR profile of LPDM

### 3.4. Optical studies

The Ultra Violet visible absorbance study of LPDM crystal exemplifies the linear optical properties. The optical absorption spectrum recorded in the region 200-700 nm is shown in Fig. 6(a). Ultra Violet visible spectral analysis gives information about electronic transitions of the compound [16]. Also it would help to understand the electronic structure and the optical band gap of the crystal. The lower optical cut-off wavelength of the LPDM crystal was found to be 259 nm, which is in the UV- region confirms the  $\pi$ - $\pi^*$  electronic transition occurrence at this region [19]. Hence this optical absorption spectrum reveals the usefulness of LPDM crystal suitability in optoelectronic applications.

The optical electronic band gap ( $E_g$ ) of the material is very closely related to the atomic and electronic band structures [16]. The optical absorption coefficient ( $\alpha$ ) was computed using the formula,

$$\alpha = \frac{2.3026 \log(1/T)}{t} \quad \text{Eq. (A.1)}$$

where T,t denotes the transmittance, thickness of the crystal. The absorption coefficient ( $\alpha$ ) was computed using the formula,

$$h\nu\alpha = A(h\nu - E_g)^{1/2} \quad \text{Eq. (A.2)}$$

In this equation A is a constant,  $E_g$  is electronic band gap energy, h is plank's constant,  $\nu$  is frequency of the incident photon. The electronic band gap energy of L-Phenylalanine D-methionine (LPDM) single crystal was evaluated from linear part of the tauc's plot by plotting  $(h\nu\alpha)^2$  versus  $h\nu$  shown in Fig. 6(b). The figure clearly shows the realization of direct allowed transition for LPDM crystal over the range 5.0-5.5 eV. The extrapolation of the straight line

down to  $(\alpha h\nu)^2 = 0$  gives the value of direct electronic band gap energy  $E_g = 5.35\text{eV}$ . Hence, this grown LPDM crystal having such wide optical band gap can be a suitable candidate for UV tunable laser and NLO device applications effectively.

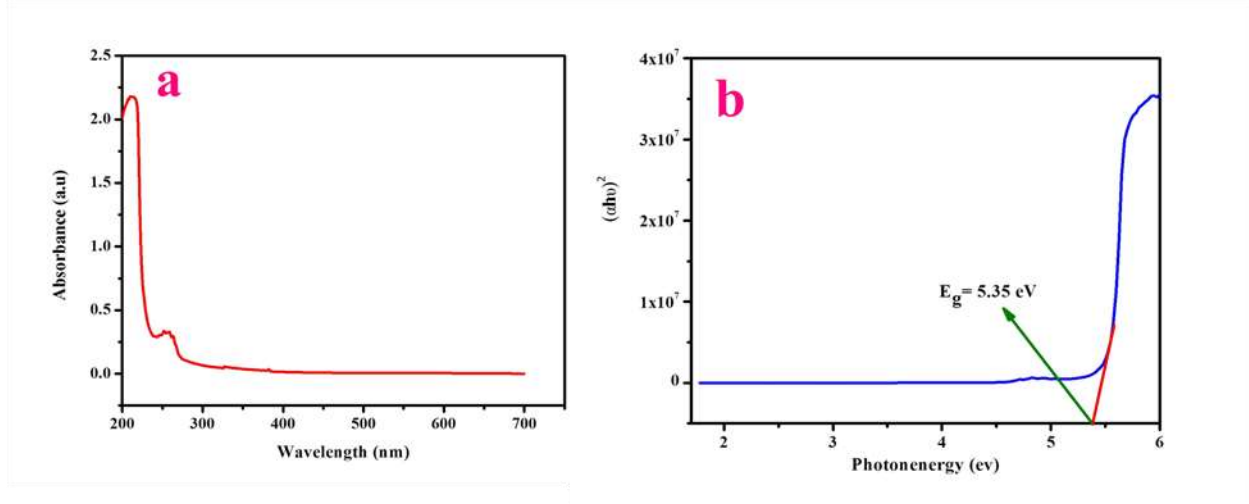


**Fig. 6.** (a) UV-vis profile and (b) Tauc's plot of LPDM.

### 3.4. 1. Determination of optical constants

The performance of a material deeply relies on the optical behaviour which forms a platform to evaluate its usage in optoelectronic devices [16]. The influence of optical absorption coefficient ( $\alpha$ ) with the high photon energy ( $h\nu$ ) helps to study the band structure and the type of transition of the electron. The different optical constants have been calculated using the following theoretical formulae [19]. Thereby absorption coefficient ( $\alpha$ ) correlated to the extinction coefficient ( $K$ ) is shown as,

$$K = \frac{\alpha \lambda}{4\pi} \quad \text{Eq. (B.1)}$$

The reflectance (R) in terms of optical absorption coefficient ( $\alpha$ ) and refractive index ( $n_x$ ) are calculated [20] and depicted in Fig. 7(a) which shows that R and K completely depend on the high photon energy [19].

$$R = 1 \pm \frac{\sqrt{1 - \exp(-\alpha t) + \exp(\alpha t)}}{1 + \exp(-\alpha t)} \quad \text{Eq. (B.2)}$$

$$n_x = - \left\{ \frac{(R+1) \pm \sqrt{3R^2 - 10R - 3}}{2(R-1)} \right\} \quad \text{Eq. (B.3)}$$

Fig. 7 (b) illustrates the twain reflectance (R) and extinction coefficient (K) dependence on absorption coefficient. The refractive index ( $n_x$ ) states that how much light is bent, or refracted, when enters the material. Since the internal efficiency of the device also controlled by the incident photon energy, by carefully tailoring the incident photon energy ( $h\nu$ ) one can aspire to have the material meant to fabricate the optoelectronic devices. Fig. 7(c) evinces the variation of refractive index ( $n_x$ ) with photon energy ( $h\nu$ ). From the figure it is clear that refractive index ( $n_x$ ) decreases with increase photon energy ( $h\nu$ ). This lowering of refractive index emphasize that the LPDM crystal exhibit the regular dispersion behaviour. The evaluated value of linear refractive index ( $n_x$ ) of 1.6373 for the LPDM crystal at 380 nm, with the high optical transparency decides LPDM as a prominent material for antireflection coating in solar thermal devices and NLO applications [19].

The photonic response due to optical conductivity ( $\sigma_{op}$ ) of the material when irradiated with light is admissible to the refractive index ( $n_x$ ) and the speed of light (c) is shown below,

$$\sigma_{op} = \frac{n_x \alpha c}{4\pi} \quad \text{Eq. (B.4)}$$

and also the electrical conductivity associated with optical conductivity of the LPDM crystal is as follows,

$$\sigma_{ele} = \frac{2\lambda\sigma_{op}}{\alpha} \quad \text{Eq. (B.5)}$$

Fig.7 (e) concludes that the optical conductivity ( $\sigma_{op}$ ) increases with photon energy ( $h\nu$ ), having high magnitude ( $10^8 \text{ } (\Omega \text{ m})^{-1}$ ) influences the presence of high photo tunable nature of the material [18]. From Fig. 7 (e) and Fig. 7 (b) it is concluded that the low extinction value ( $10^{-5}$ ) and electrical conductivity ( $1.0 \times 10^{13} \text{ } (\Omega \text{ m})^{-1}$ ) reinforce semiconducting nature of the material. Hence this material could be suitable for device applications in computing ultrafast optical data [19].

From the optical constants, the electric susceptibility ( $\chi_c$ ) could be evaluated from the following relation [19],

$$\varepsilon_r = \varepsilon_0 + 4\pi\chi_c = n_x^2 - K^2 \quad \text{Eq. (B.6)}$$

$$\chi_c = \frac{n_x^2 - K^2 - \varepsilon_0}{4\pi} \quad \text{Eq. (B.7)}$$

where  $\varepsilon_0$  is the dielectric constant in absence of any contribution from free carriers. The calculated value of electric susceptibility  $\chi_c$  is 0.2261 at  $\lambda = 380 \text{ nm}$  (Fig. 7(d)).

The real part ( $\varepsilon_r$ ) and imaginary part ( $\varepsilon_i$ ) of the dielectric constants can be rated from the following relations [19],

$$\varepsilon_r = n_x^2 - K^2 \text{ and } \varepsilon_i = 2n_xK \quad \text{Eq. (B.8)}$$

The value of real part ( $\epsilon_r$ ) and imaginary part ( $\epsilon_i$ ) of the dielectric constants at  $\lambda= 380$  nm are  $2.6806 \times 10^{-6}$  and  $17.191 \times 10^{-6}$  respectively. Hence the optical constants of a material such as electronic optical band gap and extinction coefficient are indeed quite necessary to judge the material's potential in optoelectronic applications [18].

Accepted manuscript

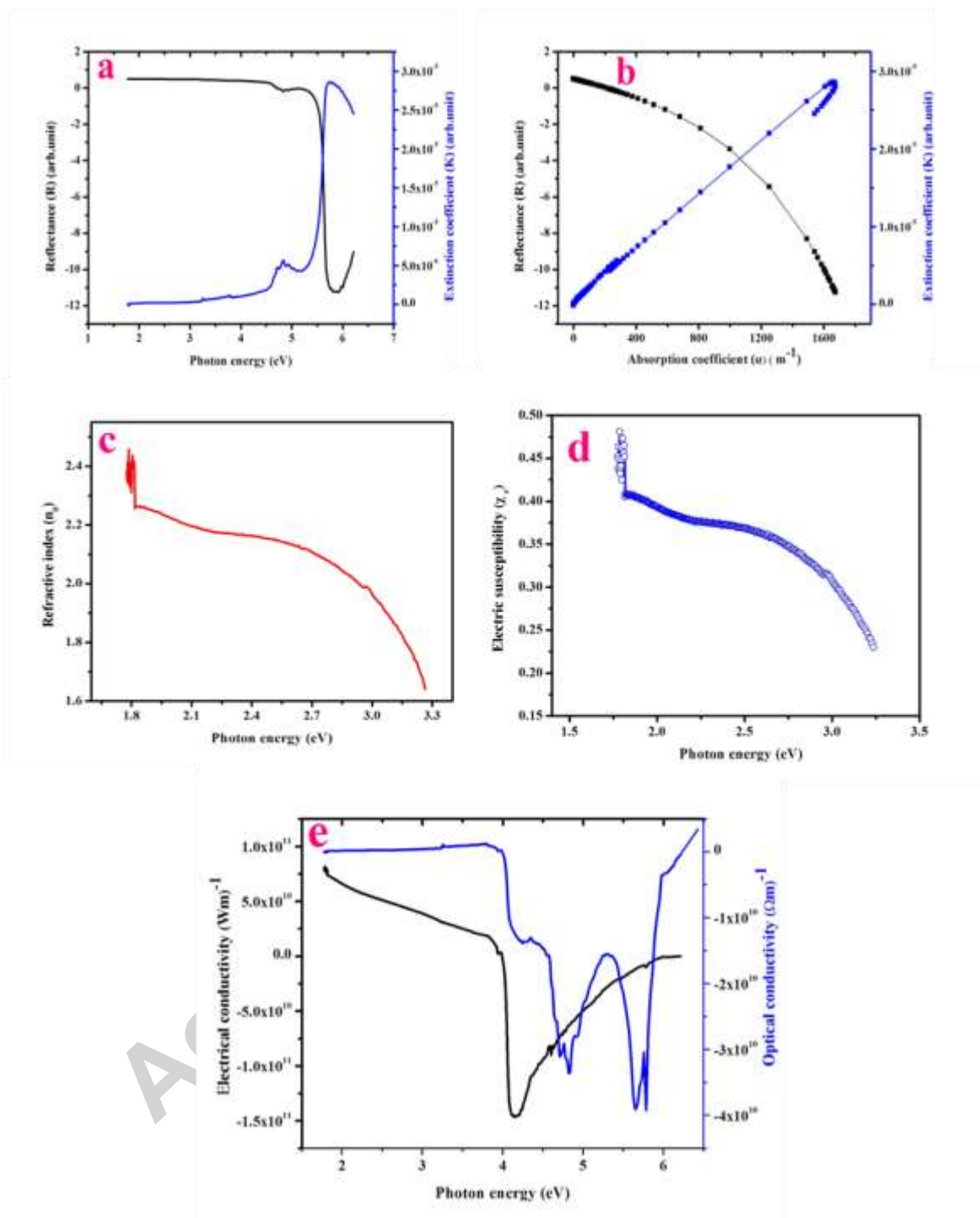


**Fig.7.** (a) Plot of reflectance (R) and extinction coefficient (K) vs. photon energy (b) Variation of reflectance (R) and extinction coefficient (K) with absorption coefficient ( $\alpha$ ) (c) Plot of refractive

index ( $n_0$ ) vs. photon energy (d) electric susceptibility ( $\chi_c$ ) vs. photon energy (e) Variation of electrical conductivity and optical conductivity vs. photon energy.

### 3.4. 2. Urbach energy

The Urbach relationship which is an exponential edge region [21] depicts the importance of absorption coefficient ( $\alpha$ ),

$$\alpha = \alpha_0 \exp\left(\frac{h\nu}{E_u}\right) \quad \text{Eq. (C.1)}$$

where  $\alpha_0$  is a constant and  $E_u$  is Urbach energy, which adhere to an indication of depth-of tail levels stretching into the forbidden electronic band gap below the absorption edge, where  $h$  is plank's constant and  $\nu$  is frequency of radiation [22]. The observed slope 7.284 of the linear portion of the plot was calculated from logarithm of the absorption coefficient ( $\alpha$ ) as a function of high photon energy ( $h\nu$ ) demonstrate that the crystal is highly crystalline in nature. Urbach energy ( $E_u$ ) was determined by taking the reciprocal of the slope of linear portion of the plot drawn between  $\ln(\alpha)$  versus  $h\nu$  as illustrated in Fig. 8. The computed Urbach energy value of 0.1372 eV being low, point out a decrease in the structural defect in as-grown LPDM crystal [23].

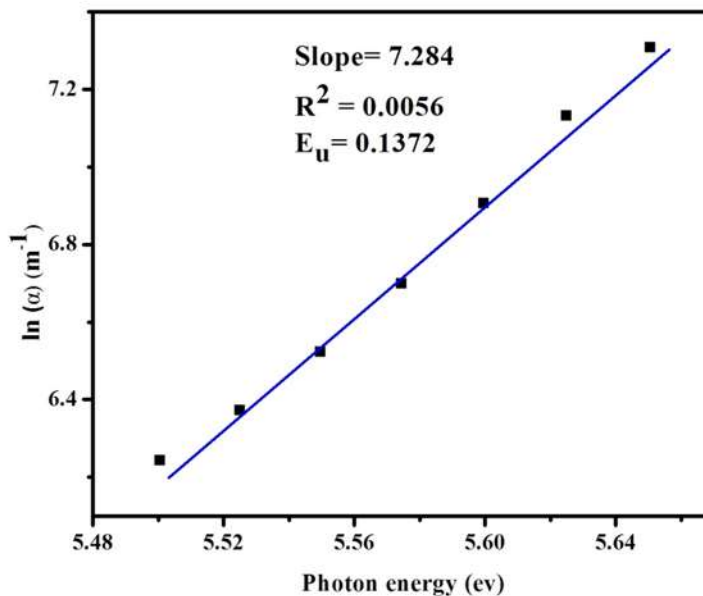


**Fig. 8 .** Plot  $\ln(\alpha)$  vs.  $h\nu$  for the LPDM

### 3.5. Thermal studies

The specimen was subjected to thermal analysis technique to estimate the weight loss (TG) and melting point (DSC) of the sample with respect to the temperature. Thermogravimetric (TGA) and differential scanning calorimetry (DSC) was conducted in an atmosphere of nitrogen at a heating rate of  $20^{\circ}\text{C min}^{-1}$  in the temperature range of 20-1000 $^{\circ}\text{C}$  are shown in Fig.9. The TGA thermogram indicates no weight loss up to 250 $^{\circ}\text{C}$ . But in the temperature region 250 $^{\circ}\text{C}$ -990 $^{\circ}\text{C}$  weight loss occurs in three steps, one starting from 250 $^{\circ}\text{C}$  and ends at 275 $^{\circ}\text{C}$  and second weight loss occur between 275 $^{\circ}\text{C}$ -375 $^{\circ}\text{C}$  shows a decrease from 55% to 20% respectively, could be due to the decomposition process. In the third stage at a temperature of about 400 $^{\circ}\text{C}$  to 990 $^{\circ}\text{C}$ , almost the compound is completely decomposed (weight loss 10%) leaving only the residue. The DSC trace of the crystal exhibits sharp exothermic peak at 268 $^{\circ}\text{C}$  is

attributed to the melting of the material, which coincides well with the TG-trace. This temperature of melting is the maximum temperature applicable for NLO applications.

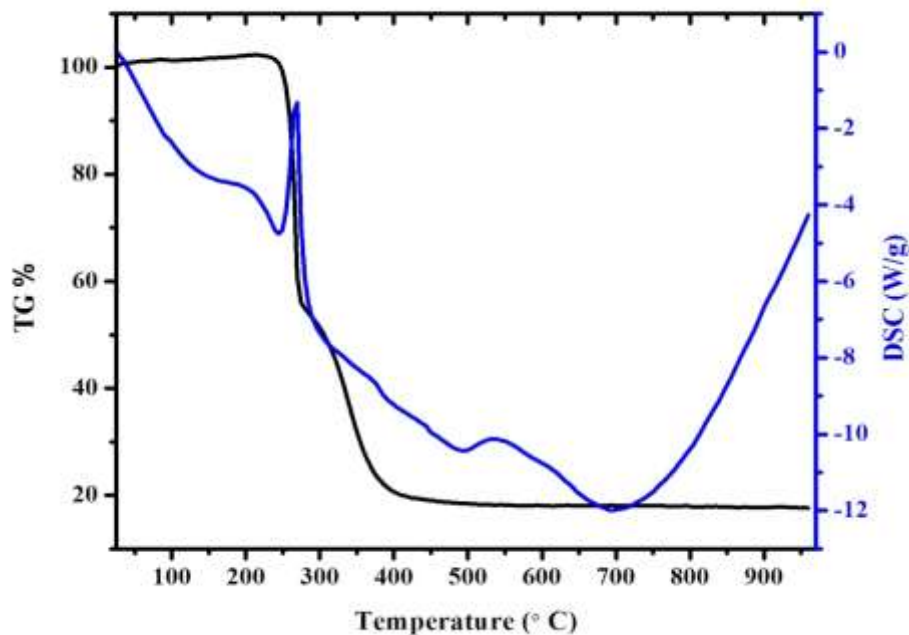


**Fig. 9.** TG-DSC profile of LPDM

### 3.6. Dielectric studies

The electrical response, molecular anisotropy, structural changes, polarization mechanism and transport phenomena within crystalline materials were analysed by dielectric measurements [24]. The dielectric constant and dielectric loss of the grown LPDM crystal was carried out for various temperatures 313 K, 333K, 353 K and 373 K in the frequency range 50 Hz to 5MHz. The dielectric constant ( $\epsilon'$ ) and dielectric loss ( $\epsilon''$ ) of LPDM were calculated using the following equation:

$$\epsilon' = \frac{Ct}{A\epsilon_0} \quad \text{Eq. (C.1)}$$

and

$$\varepsilon'' = \varepsilon' \tan \delta \quad \text{Eq. (C.2)}$$

respectively. Where C is the capacitance in  $\mu\text{F}$ , t is the thickness of the sample in mm,  $\varepsilon_0$  is the vacuum dielectric constant ( $\varepsilon_0 = 8.854 \times 10^{-12} \text{ Fm}^{-1}$ ), A- Area of the sample in  $\text{mm}^2$  and  $\tan \delta$  is the dissipation factor. From Fig. 10 (a) and 10 (b) it is spotted that increase of frequency there is a decrease of dielectric constant and dielectric loss. The large values of ( $\varepsilon'$ ) at low frequencies is due to the outcome of the contribution of all the four polarizations namely electronic, space charge, orientation and ionic polarization. Also the low value of ( $\varepsilon'$ ) at high frequency region is triggered by inability of the dipoles in consent with the external field [18]. Thus, the attributed very low value of dielectric constant and dielectric loss at higher frequencies divulge the enhanced optical quality with defect less LPDM crystal, in order to meet the requirements in opto-electronic applications and photonic applications [24].

### 3. 6. 1. A.C conductivity

The a.c conductivity  $\sigma_{ac} (\Omega \text{ m})^{-1}$  has been calculated from the following formula:

$$\sigma_{ac} = 2\pi f \varepsilon_0 \varepsilon' \tan \delta \quad \text{Eq. (D.1)}$$

where f is the applied frequency of ac field (Hz). The variation of  $\log \omega$  with ac conductivity at various temperatures has been plotted and shown in Fig. 12(c).

### 3. 6. 2. Activation energy

The activation energy ( $E_a$ ) is evaluated using the following relation:

$$\sigma = \sigma_0 \exp\left(-\frac{E_a}{k_B T}\right) \quad \text{Eq. (E.1)}$$

Where  $\sigma_{ac}$  is the conductivity at temperature  $T$ ,  $E_a$  - activation energy,  $k_B$  is the Boltzmann constant ( $k_B = 1.38 \times 10^{-23}$  J/K). Fig. 12(d) shows the variation of  $\log \sigma_{ac}$  versus  $1000/T$ . This is almost linear in behavior and the slope of this graph is used to estimate the activation energy ( $E_a$ ) using the relation,

$$E_a = -\text{slope} \times 1000 \times k_B \quad \text{Eq. (F.2)}$$

The value of the activation energy comes out to be 0.00270, 0.00732, 0.00858 and 0.01997 eV at frequencies 4 KHz, 100 KHz, 2 MHz and 5 MHz respectively evince that LPDM possesses less defect owing to less value of activation energy. Flawless crystals become more useful materials for device fabrications [19].

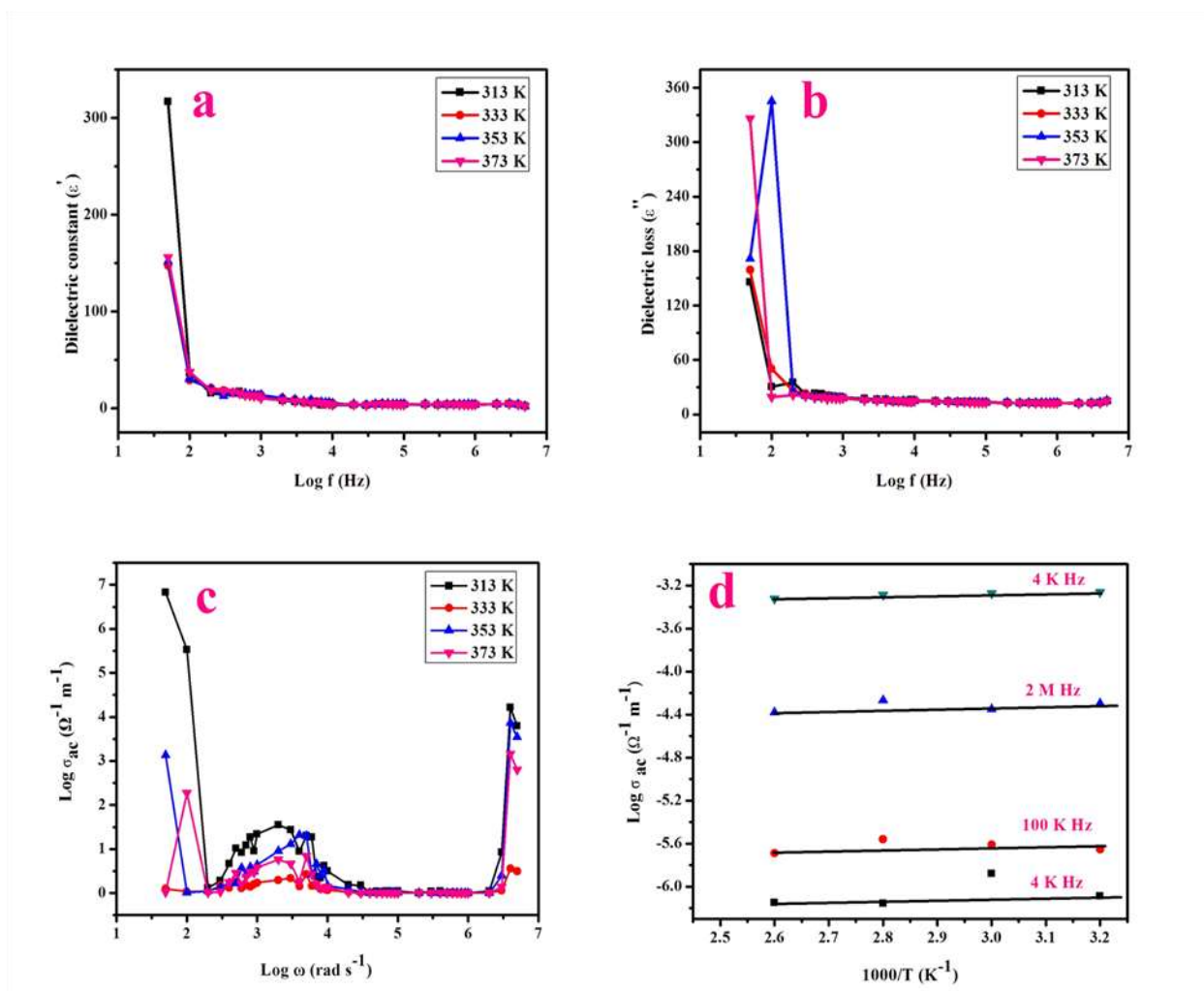


**Fig.10.** Plot of (a)  $\text{Log } f$  vs. dielectric constant (b)  $\text{Log } f$  vs. dielectric loss (c)  $\text{Log } \sigma_{ac}$  vs.  $\text{log } \omega$  and (d)  $\text{Log } \sigma_{ac}$  vs.  $1000/T$ .

### 3. 7. Fluorescence and life time measurement

The fluorescence profile (Fig. 11(a)) of LPDM crystal at excitation wavelength 259 nm was studied to outlook over the emission spectrum in regard with that particular excited state of the system and decaying components [24]. The emission peaks with maximum intensity is found occurring at 284 nm (4.37 eV), which is just near to the visible region in accordance with the electromagnetic spectrum. The existence of 2-day (prompt and delayed) component of fluorescence materials paves the way to neutron-gamma discrimination. A distinctive feature of

the organic scintillator as a detector application is to manifest various lifetime at the same emission wavelength. The lifetime quantification was performed with the help of FLUOROCUBE spectrofluorometer with the wavelength of 284 nm. The lifetime profile was evaluated by adopting time-correlated single photon counting method (TCSPC) [24]. Fig. 11(b) represents the three exponential decay time profiles for the LPDM single crystal. The analysis of decay time measurement was fitted with a three exponential decay function is of the form,

$$F(t) = A_1e^{-t/\tau_1} + A_2e^{-t/\tau_2} + A_3e^{-t/\tau_3} \quad \text{Eq. (G.1)}$$

Where  $A_1$ ,  $A_2$  and  $A_3$  denotes amplitudes and  $\tau_1$ ,  $\tau_2$  and  $\tau_3$  are lifetimes of prompt and delayed emissions. The residual fit presented in Fig.11(c) specifies the extent of best fitting done to the actual decay curve. The quality of the curve fit was accomplished by the inspection of the residuals, and the value of the reduced  $\chi^2$  ratio. For the organic molecular crystals the fast scintillation decay time lies in between 2 and 30 ns [24]. The present study exhibited the shortest decay component which is detailed in Table 2.

**Table 2**

Fluorescence lifetime analysis data of LPDM crystal.

Single crystal	Analysis	Lifetime (ns)			Amplitude			$\chi^2$
		$\tau_1$	$\tau_2$	$\tau_3$	$A_1$	$A_2$	$A_3$	
LPDM	Three exponential	2	7	9	43.85	32.52	23.62	1.06

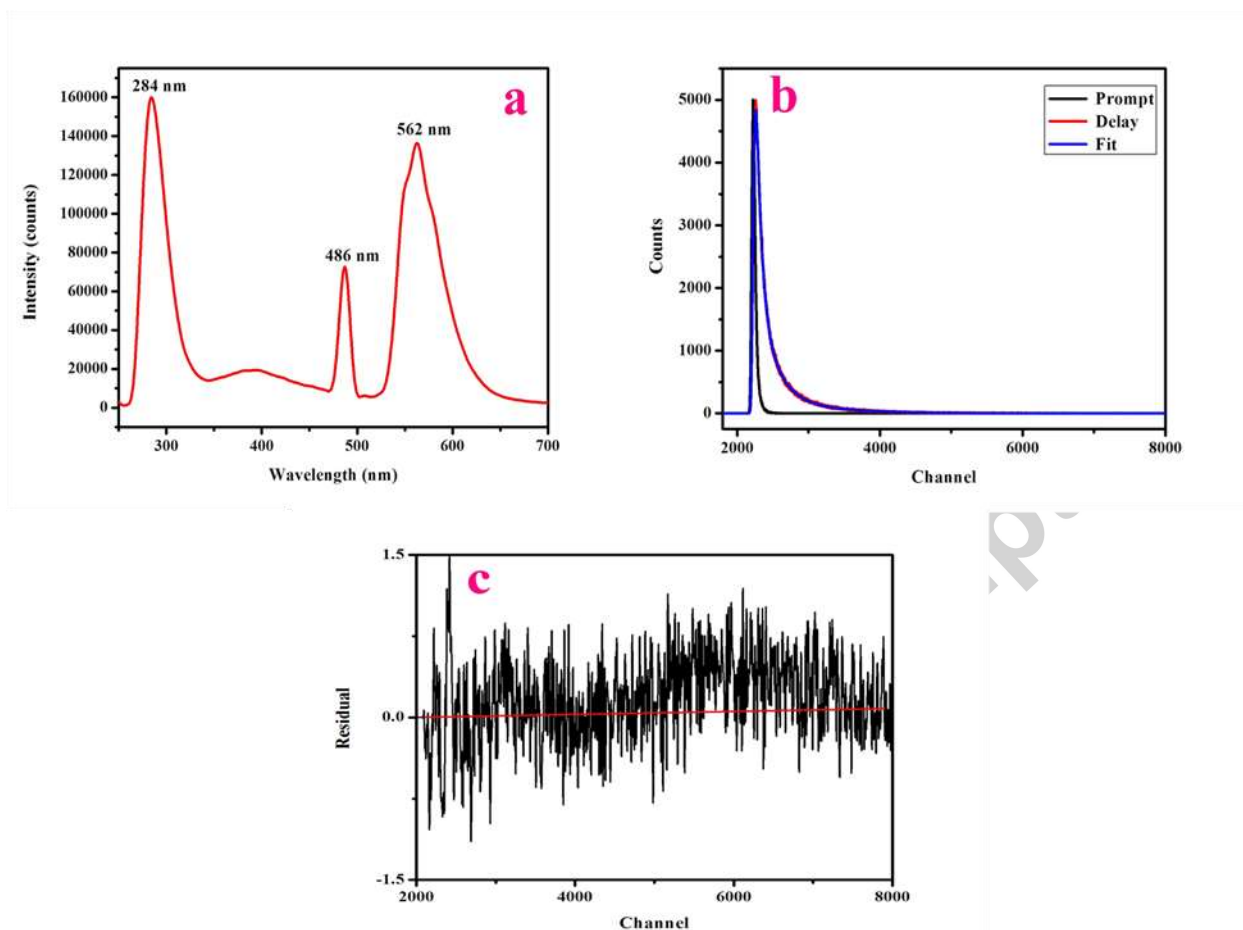


**Fig.11.** (a) Emission spectrum (b) Fluorescence lifetime spectrum (c) Residual fit of LPDM.

### 3.8. SEM analysis

The surface investigation was performed using FE1 quanta FEG 200 High resolution scanning electron microscope with acceleration voltage of 30KV and the sample is kept at high vacuum. Fig.13(a,b,c,) represents the recorded SEM micrograph of LPDM crystal with resolutions 30000 X, 20000 X, 16000 X respectively reveal the layers of atoms of different sizes and also portrays the surface of the microcrystal as sharp fine morphology free from cracks. The overlapping of crystals occurred due to agglomeration effected by the thermal effect during synthesis process.

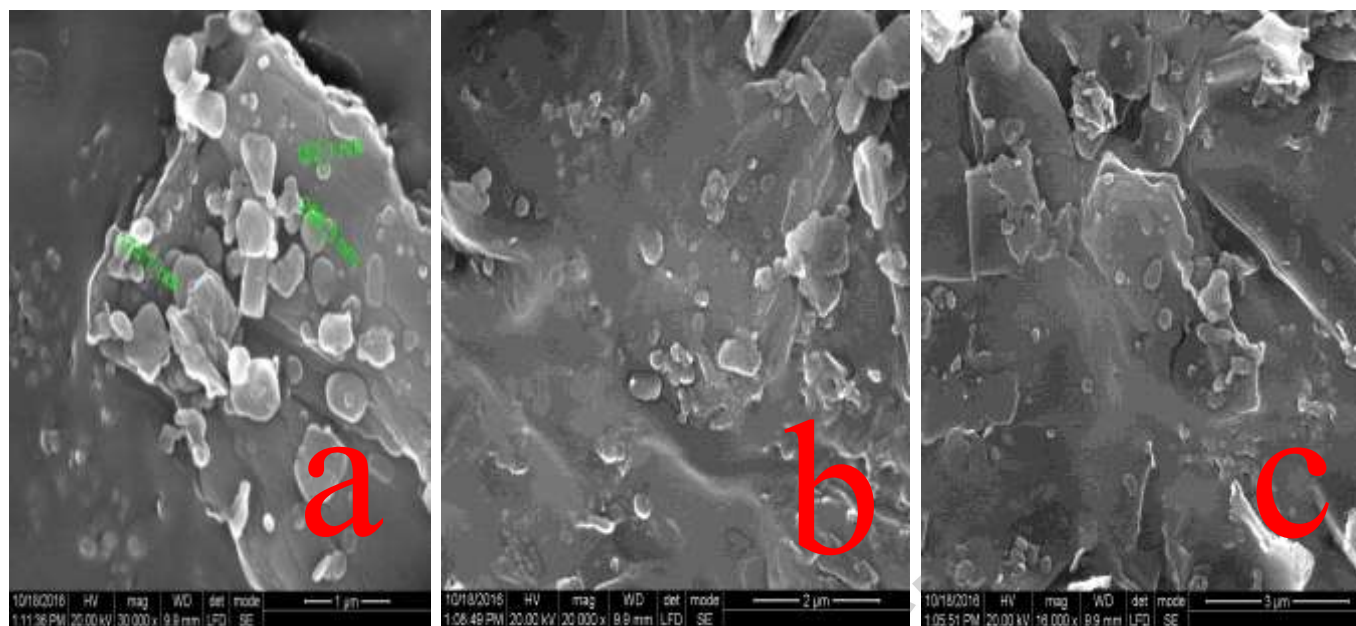


**Fig. 12(a,b,c). SEM Micrograph of LPDM crystal at a resolution of 30000 X,20000 X,16000 X with (a)1  $\mu\text{m}$  (b)2  $\mu\text{m}$  (c) and 3  $\mu\text{m}$**

### 3.9. NLO studies

The second harmonic generation (SHG) conversion efficiency was individualized by the Kurtz-Perry powder method [25], and the efficiency of the sample was correlated with the microcrystalline powder of  $\text{KH}_2\text{PO}_4$  (KDP). In this method the sample made into a very fine powder with average particle size of 100-115 $\mu\text{m}$  was tightly packed in a microcapillary tube, and illuminated using spectra physics quanta Nd:YAG laser emitting a first harmonic output of 1064 nm with the pulse width of 10 ns. The input laser beam energy 0.69 J was passed through the IR reflector and then aimed on the microcrystalline powder sample of KDP. The frequency-doubled output pulse values of 8.91 mJ and 5.72 mJ were obtained for KDP and LPDM respectively. The KDP was used as the reference material and the second harmonic generation conversion efficiency of the LPDM was found to be 0.64 times that of KDP. Some of the reported organic noncentrosymmetric chromospheres with space group and NLO efficiency are listed in Table 3 for comparison. Hence the wavelength conversion efficiency in LPDM

concludes it as a suitable candidate to develop NLO devices such as optical communication system.

**Table 3**

Comparison of NLO efficiency of non-centrosymmetric crystals.

Crystal	spacegroup	NLO efficiency	Reference
L-phenylalanine nitric acid	P2 <sub>1</sub>	0.26	[14]
L-alanine	P2 <sub>1</sub>	0.33	[6]
L-phenylalanine dl-mandelic acid	C2	0.35	[16]
<b>L-phenylalanine D-methionine</b>	<b>P2<sub>1</sub></b>	<b>0.64</b>	<b>[Present work]</b>

### 3.10. Z -Scan studies

The third-order optical nonlinearities have been evaluated for the organic LPDM material by the THG measurement using single beam Z-scan technique equipped with He-Ne laser of intensity 5 mW ( $\lambda = 632.8$  nm), focused by a lens of 3.5 cm focal length. It is a simple and highly sensitive but very accurate method to determine nonlinear index of refraction ( $n_0$ ), nonlinear absorption coefficient ( $\beta$ ) and third-order nonlinear optical susceptibility ( $\chi^{(3)}$ ) by closed and open aperture mode respectively [24]. Measurement of the closed aperture, open aperture and ratio of the closed-to-open normalized transmittance as a function of sample position Z have been done for LPDM crystal and illustrated in Fig. 13 (a), (b) and (c). In closed aperture pattern (Fig. 13(a)), we could see that the peak followed by a valley intensity, signifies that the sign of the refraction nonlinearity is negative, i.e., the occurrence of self-defocusing effect [23]. The open aperture Z-scan sign (Fig. 13(b)) suggests that the sample exhibits saturable

absorption. The measurable quantity ( $\Delta T_{p-v}$ ) can be defined as the difference between the transmittance change of peak and valley  $T_p - T_v$ . The on-axis phase shift at the focus  $|\Delta\Phi_0|$  is given by,

$$\Delta T_{p-v} = 0.406(1-S)^{0.25}|\Delta\Phi_0| \quad \text{Eq. (H.1)}$$

$$S = 1 - \exp\left(\frac{-2r_a^2}{\omega_a^2}\right) \quad \text{Eq. (H.2)}$$

where  $S$  is the linear transmittance aperture,  $r_a$  denoting the radius of the aperture and  $\omega_a$  is the beam radius at the aperture. The on-axis phase shift  $|\Delta\Phi_0|$  is related to the third-order nonlinear refractive index of the crystal by,

$$n_2 = \frac{\Delta\Phi_0}{KI_0L_{eff}} \quad \text{Eq. (H.3)}$$

where  $I_0$  is the intensity of the laser beam at focus ( $Z=0$ ) and  $L_{eff}$  is the effective thickness of the sample which can be evaluated by using the relation  $L_{eff} = [1 - \exp(-\alpha L)] / \alpha$ , where  $\alpha$  and  $L$  is the linear absorption coefficient and the thickness of the sample respectively. From the open aperture curve, the nonlinear absorption coefficient ( $\beta$ ) can be obtained using the relation,

$$\beta = \frac{2\sqrt{2}\Delta T}{I_0L_{eff}} \quad \text{Eq. (H.4)}$$

where  $\Delta T$  is the one valley value at the open aperture  $Z$ -scan trace. The value of  $\beta$  is negative for saturated absorption and positive for two-photon absorption processes [23]. The experimental determination values of  $n_2$  and  $\beta$  were used to estimate the real and imaginary parts of the third-order nonlinear optical susceptibility:

$$\text{Re } \chi^{(3)}(\text{esu}) = \frac{10^{-4}(\varepsilon_0 C^2 n_o^2 n_2)}{\pi} \left( \frac{\text{cm}^2}{\text{W}} \right) \quad \text{Eq. (H.5)}$$

$$\text{Im } \chi^{(3)}(\text{esu}) = \frac{10^{-2}(\varepsilon_0 C^2 n_o \lambda \beta)}{4\pi^2} \left( \frac{\text{cm}^2}{\text{W}} \right) \quad \text{Eq. (H.6)}$$

where  $\varepsilon_0$  is the permittivity of free space ( $8.8518 \times 10^{-12} \text{Fm}^{-1}$ ),  $C$  is the velocity of the light in a vacuum and  $n_0$  is the linear refractive index of the crystal. The absolute value of third-order nonlinear optical susceptibility  $\chi^{(3)}$  was calculated according to the following relation,

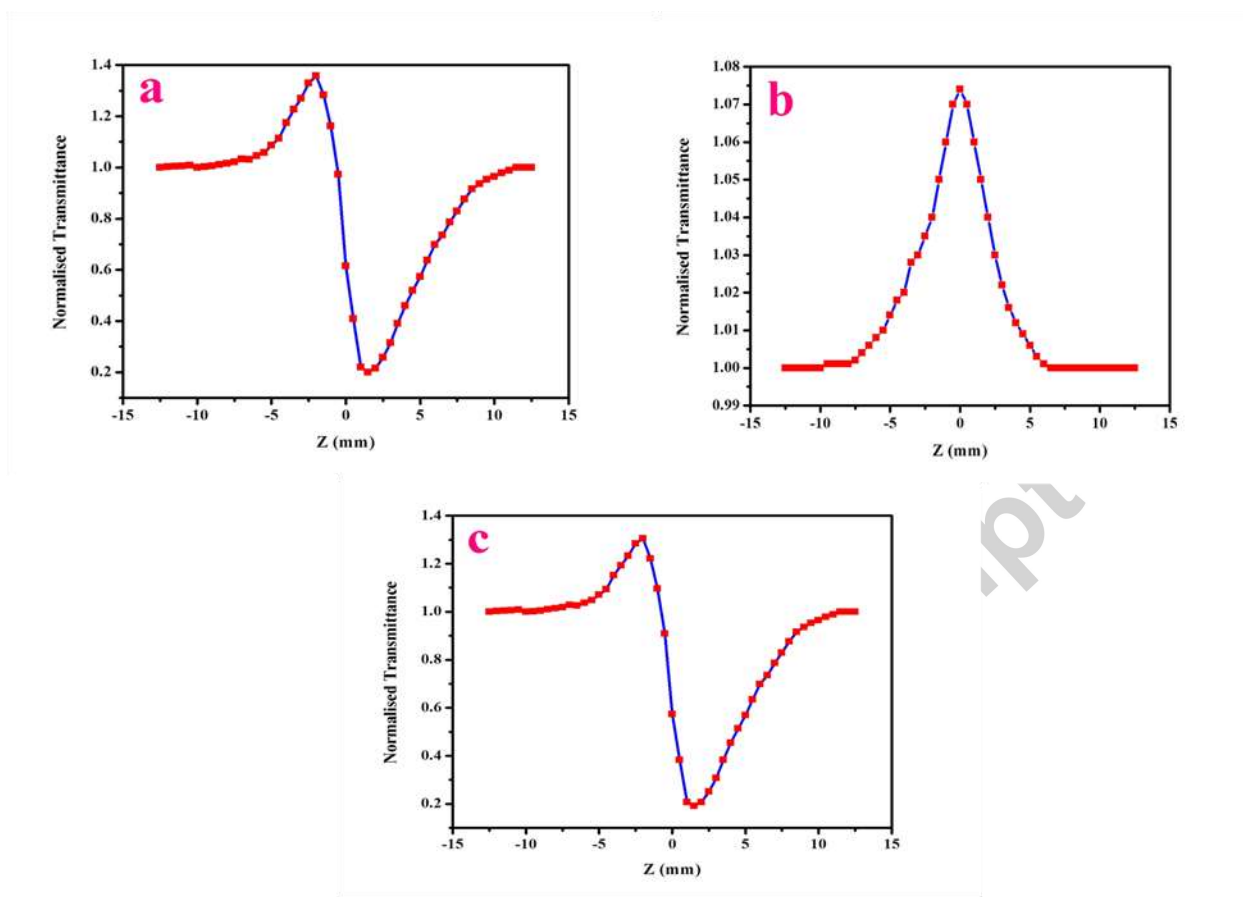
$$|\chi^{(3)}| = \sqrt{(\text{Re}(\chi^{(3)}))^2 + (\text{Im}(\chi^{(3)}))^2} \quad \text{Eq. (H.7)}$$

Table 3 personate the experimental details and the results of the Z-scan technique for LPDM crystal. Thus, the LPDM could be a suitable candidate for the protection of night vision optical sensors, optical limiting applications [24].

**Table 4**

Obtained nonlinear optical parameters from Z-scan measurements for LPDM.

Parameters	Measured values for LPDM crystal
Laser beam wavelength ( $\lambda$ )	532 nm
Linear absorption coefficient ( $\alpha$ )	237.94
Nonlinear refractive index ( $n_2$ )	$5.77 \times 10^{-8} \text{cm}^2 \text{W}^{-1}$
Nonlinear absorption coefficient ( $\beta$ )	$0.050 \times 10^{-4} \text{cmW}^{-1}$
Real part of the third-order susceptibility [ $\text{Re}(\chi^3)$ ]	$3.08 \times 10^{-6} \text{esu}$
Imaginary part of the third-order susceptibility [ $\text{Im}(\chi^3)$ ]	$0.34 \times 10^{-6} \text{esu}$
Third-order nonlinear optical susceptibility ( $\chi^3$ )	$3.10 \times 10^{-6} \text{esu}$



**Fig. 13.** (a) Closed aperture (b) Open aperture and (c) Ratio of the closed-to-open Z-scan traces of LPDM.

## Conclusion

Organic chromophore LPDM was synthesized and good quality crystals were grown by the slow solvent evaporation solution growth technique. The cell parameters and crystal structure of LPDM were examined by single crystal XRD. The presence of functional groups was identified by FTIR and FT-Raman spectral analyses. The Nuclear Magnetic Resonance (NMR) analysis identifies the functional groups that contribute the grown crystal. The UV-vis spectra of the LPDM crystals showed that they are highly transparent in nature in the visible region, with the cut-off wavelength at 259 nm. The calculated optical direct band-gap value was evaluated to be 5.13 eV using Tauc's plot. Optical parameters such as absorption coefficient ( $\alpha$ ), reflectance

(R), extinction coefficient (K) refractive index ( $n_0$ ), electric susceptibility ( $\chi_c$ ) and optical conductivity ( $\sigma_{op}$ ) were calculated to analyze the optical properties. TG-DSC analyses illustrate that the compound is thermally stable up to 268°C. From the dielectric studies supporting parameters like a.c conductivity ( $\sigma_{ac}$ ) and activation energy ( $E_a$ ) were evaluated divulge presence of less number of defects in the as-grown crystal. Fluorescence lifetime is estimated as  $\tau_1=2$ ,  $\tau_2=7$  and  $\tau_3=9$  ns. SEM images display the layers of atoms of different sizes and its surface have a smooth topography in nature. The nonlinear optical test reveals that LPDM exhibit SHG efficiency of 0.64 times that of  $KH_2PO_4$  (KDP). Closed aperture Z-scan study reveal negative nonlinearity (self-defocusing) in the LPDM crystal and open aperture Z-scan reveals the reverse saturation absorption. The studies carried out conclude that LPDM is a potential candidate for perspective use in future optical limiting and nonlinear optical devices fabrication.

### Acknowledgements

The authors (M.L and P.S) thank the scientific supports extended by sophisticated analytical instruments facility (SAIF), Indian Institute of Technology (IITM) for providing single crystal XRD, FTIR, FT-Raman, NMR and thermal analysis measurement.

### References

- [1] K. Thukral, N. Vijayan, B.K. Singh, I. Bdikin, D. Haranath, K.K. Maurya, J. Philip, H. Saumya, P. Sreekanth, G. Bhagavannaranya, Growth, structural and mechanical analysis of L-prolinium tartrate single crystal: A promising Materials for nonlinear optical Applications, RSC Cryst. Eng. Commu. (2014) DOI: 10.1039/C4CEO1232A.

- [2] S.Natarajan, N.R.Devi, S.A.Martin Britto Dhas, S.Athimoolam, Growth, thermal and optical studies of a new organic NLO materials: L-methionine L-methioninium hydrogen maleate, optoelect. and Adv.Mat.4 (2010) 516-519.
- [3] W.Srimahaprom, Adrian E.Flood, Crystal growth rates and optical resolution of DL-methionine hydrochloride by preferential crystallization from aqueous solution J. Crys.Growth. 362 (2013) 88-92.
- [4] R.A.Moats, K.D.Moselay, R.Koch, M.Nelson Jr.Brain, Phenylalanine in Phenylkentonuria: Research and Treatment of Adults, Pediatrics 2003.
- [5] M. Prakash, D. Geetha, M.Lydia Caroline, Crystal growth and Characterization of L-Phenylalaninium trichloroacetate, A new organic nonlinear optical material, Physica B 406 (2011) 2621-2625.
- [6] M. Lydia Caroline, R. Sankar, R.M. Indirani, S. Vasudevan, Growth, optical, thermal and dielectric studies of an amino acid organic nonlinear optical material:L-alanine, Mater. Chem and Phys. 114 (2009) 490-494.
- [7] M. Prakash, D. Geetha, M. Lydia Caroline, Crystal growth, structural, optical, spectral and thermal studies of tris(l-phenylalanine)l-phenylalaninium nitrate: A new organic nonlinear optical material, Spectrochim. Acta Part A 81 (2011) 48-52.
- [8] Osamu Yamamoto, Radiation-induced binding of methionine with serum albumin, Tryptophan or phenylalanine in aqueous solution, Int.J.Radiation.Phys.Chem. 4. (1972) 335-345.
- [9] C.H.Gorbitz ,Peptide structures, Solid State and Materials Science 6 (2002) 109-116.

- [10] C.H.Gorbitz, K.Rissanen, A.Valkonan and A.Hussabo, Molecular aggregation in selected crystalline 1:1 complexes of hydrophobic D and L-amino acids .IV. The phenylalanine series, *Acta Cryst.*c65, o267-o272.
- [11] D. J. Williams, Ed., “Nonlinear Optical Properties of Organic and Polymeric Materials,” ACS Symposium Ser. 233, Washington D.C., 1983.
- [12] Chemla D.S. and Zyss J. (1987), ‘Nonlinear optical properties of organic molecules and crystals’, Academic Press, Orlando, New York, Vol. 1-2.
- [13] K. Kubodera and H. Kobayashi, Determination of Nonlinear optical susceptibilities for organic materials by third-harmonic generation, *Mol.Cryst.Liq.Cryst.* 182 (1990) 103-113.
- [14] M.Lydia Caroline, S.Vasudevan, Growth and characterization of L-phenylalanine nitric acid, a new organic nonlinear optical material,*Mater.Lett.*63 (2009) 41-44.
- [15] M. Prakash, D. Geetha, M. Lydia Caroline, Growth and characterization of Nonlinear Optics (NLO) active L-phenylalanine fumaric acid (LPFA) single crystal, *Materials and Manufacturing processes*, Taylor & Francis 27 (2012) 519-522.
- [16]P.Jayaprakash,M.PeerMohamed,P.Krishnan,M.Nageshwari,G.Mani,M.LydiaCaroline, Growth, spectral, thermal, laser damage threshold, microhardness, dielectric, linear and nonlinear optical properties of an organic single crystal: L-Phenylalanine DL-mandelic acid, *Physica B* 503 (2016) 25-31.
- [17] George Socrates, *Infrared and Raman Characteristic Group Frequencies*, John Wiley & Sons Publishers, 3<sup>rd</sup> ed., England, 2001.

- [18] M. Peer Mohamed, P. Jayaprakash, M. Nageshwari, C. Rathika Thaya Kumari, P. Sangeetha, S. Sudha, G. Mani, M. Lydia Caroline, Crystal growth, structural, spectral, thermal, linear and nonlinear optical characterization of a new organic nonlinear chiral compound: L-tryptophan-fumaric acid-water (1/1/1) suitable for laser frequency conversion J. Mol. Struct. 1141 (2017) 551-562.
- [19] P. Jayaprakash, M. Peer Mohamed, M. Lydia Caroline, Growth, spectral and optical characterization of a novel nonlinear optical organic material: D-Alanine DL-Mandelic acid single crystal, J. Mol. Struct. 1134 (2016) 67-77.
- [20] R. Surekha, R. Gunaseelan, P. Sagayaraj, K. Ambujam, L-phenylalanine l-phenylalaninium bromide-a new nonlinear optical material, The Roy. Soc. Chem. 16 (2014) 7979-7989.
- [21] F. Urbach, The long-wavelength edge of photographic sensitivity and of the electronic absorption of solids, Phys. Rev. 92 (1953) 1324.
- [22] M.D. Migahed, H.M. Zidan, Influence of UV-irradiation on the structure and optical properties of polycarbonate films, Curr. App. Phy. 6 (2006) 91.
- [23] M. Nageshwari, P. Jayaprakash, C. Rathika Thaya Kumari, G. Vinitha M. Lydia Caroline, Growth, spectral, linear and nonlinear, optical characteristics of an efficient semiorganic acentric crystal: L-valinium L-valine chloride, Physica B 511 (2017) 1-9.
- [24] P. Jayaprakash, P. Sangeetha, C. Rathika Thaya Kumari, M. Lydia Caroline, Investigation on the growth, spectral, lifetime, mechanical analysis and third-order nonlinear optical studies of L-methionine admixture D-mandelic acid single crystal: a promising material for nonlinear optical applications, Physica B 518 (2017) 1-12.

[25] S.K. Kurtz, T.T. Perry, A powder technique for the evaluation of nonlinear optical materials, J. Appl. Phys. 39 (1968) 3798-3813.

### Table captions

**Table 1** Single crystal XRD crystallographic data of LPDM.

**Table 2** Fluorescence lifetime analysis data of LPDM crystal.

**Table 3** Comparison of NLO efficiency of non-centrosymmetric crystals.

**Table 4** Obtained nonlinear optical parameters from Z-scan measurements for LPDM.

### Figure captions

**Fig.1.** Reaction scheme for LPDM compound.

**Fig. 2.** The grown LPDM crystals.

**Fig. 3.** (a) FTIR (b) FT-Raman profile of LPDM.

**Fig. 4.**  $^1\text{H}$  NMR profile of LPDM.

**Fig. 5.**  $^{13}\text{C}$  NMR profile of LPDM.

**Fig. 6.** (a) UV-vis profile and (b) Tauc's plot of LPDM.

**Fig. 7.** (a) Plot of reflectance (R) and extinction coefficient (K) vs. photon energy (b) Variation of reflectance (R) and extinction coefficient (K) with absorption coefficient ( $\alpha$ ) (c) Plot of refractive index ( $n_0$ ) vs. photon energy (d) electric susceptibility ( $\chi_c$ ) vs. photon energy (e) Variation of electrical conductivity and optical conductivity vs. photon energy.

**Fig. 8.** Plot  $\ln(\alpha)$  vs.  $h\nu$  for the LPDM.

**Fig. 9.** TG-DSC profile of LPDM.

**Fig.10.** Plot of (a) Log f vs. dielectric constant (b) Log f vs. dielectric loss (c) Log  $\sigma_{ac}$  vs. log  $\omega$  and (d) Log  $\sigma_{ac}$  vs.  $1000/T$ .

**Fig.11.** (a) Emission spectrum (b) Fluorescence lifetime spectrum (c) Residual fit of LPDM.

**Fig. 12 (a,b,c).** SEM Micrograph of LPDM crystal at a resolution of 30000 X,20000 X,16000 X with (a)1  $\mu\text{m}$  (b)2  $\mu\text{m}$  (c) and 3  $\mu\text{m}$ .

**Fig.13.** (a) Closed aperture (b) Open aperture and (c) Ratio of the closed-to-open Z-scan traces of LPDM

Accepted manuscript